한국지리정보학회지 2권 2호 : 45~58(1999)

Distributions of Hydrogeological Variables and Flow Field on GIS Digital Map

Cheo K. Lee[1]

GIS 수치지도를 이용한 수리지질학적 변수와 지하수 유동의 분포

이처경[1]

ABSTRACT

Digital map is utilized for an effective display of the distributions of the hydrogeological variables such as water table height(hydraulic head) and log-transmissivity($\ln T$) in north Pohang, KyungBug. Specifically the geostatistical method kriging is used to construct the distributions in an unconfined aquifer from a finite set of measured data. The experimental variograms for both the head and $\ln T$ suggest spherical models with nugget of 0 and range of 6km. The kriged results by using these variograms show that the head decreases primarily from the west to the east with a large peak in the north-western part and $\ln T$ is at the maximum level in the central part with outwardly decreasing trend. The constructed delineation is also used to calculate the flow field in the region. Finite differences with second order consistency are used to calculate the fluxes in the east(x) and north (y) across a vertical cross-section of unit width and height equal to the thickness of the wet zone in the aquifer. It is demonstrated that the flow is dominantly in the east with diverging trend on the eastern hillside of the water table peak. A few convergent spots also appear.

KEYWORDS: Digital Map, Groundwater, Hyudraulic Head, Transmissivity, Kriging

요 약

경북 포항 북부 지역의 지하수면고도(수두)와 로그-투수량계수의 분포 상황을 효과적으로 나타내기 위해 수치지도를 활용하였다. 특히 분포 상황 구현을 위해 자연 지하수층내의 유한한 측정치들에 지하탐사 통계학적 방법 kriging을 이용하였다. 계산된 variogram들은 spherical model로 근사하였으며 nugget과 range는 각각 0과 6km로 취하였다. 수두의 분포는 북서쪽의 peak로부터 대체로 동쪽 방향으로 낮아지며, 로그-투수량계수는 중심부근에서 최대값을 보이고 외곽쪽으로 감소한다. 지하수면고도와 로그 투수량계수의 분포로부터 지하수의 동쪽 및 북쪽 방향 유량을 유한차분법을 이용하여 계산하였다. 유동의 방향은 peak로부터 대체로 동향이고 peak의 동쪽방면에서 발산하는 경향을 보인다. 지역내의 몇 지점에서는 수렴하는 유동이 나타나기도 한다.

주요어: 수치지도, 지하수, 수두, 투수량계수, 크리깅

1999년 8월 6일 접수 Received on August 6, 1999
1 한동대학교 건설도시환경공학부 (cklee@han.ac.kr)
School of Construction and Urban Environmental Engineering, Handong University

INTRODUCTION

In order to set up a reliable plan for efficient management of groundwater resources, a fairly good understanding of the spatial distribution of groundwater reserve should be achieved in terms of several hydrogeological characteristics. It is also important to effectively display the distribution of hydrogeological variables. For this purpose digital map is utilized which contains the contours of the ground surface elevation, and the main roads and streams. The advantages of using digital map are two-fold. First, by providing the distribution of the variables, locations for future development of ground water can be conveniently identified in connection with existing geographic information. Second, areas of possible ground water contamination due to infiltrated pollutants and flowing water can be easily identified in the region of interest.

Groundwater is a valuable water resource which, if managed by an efficient scheme, can be repeatedly used for various water-demanding purposes. As the level of pollution in the surface water becomes quite alarming, the groundwater is receiving ever more attention with special regards to the feasibility for development and its conservation. It is known that the groundwater is moving, although very slow, continually in the subsurface environment usually at the rate of a few tens of centimeters per day. The movement is described by Darcy's law which states that the water flux per unit cross-sectional area is linearly proportional to the hydraulic conductivity and the hydraulic gradient which is simply the rate of change of the hydraulic head in space (Bear, 1972).

In an unconfined (phreatic) aquifer, the hydraulic head is equivalent to the water table height measured from a horizontal datum level. For a description of the flow field, it is necessary to construct the distribution of the water table height. Also required is the hydraulic conductivity whose distribution is, in reality, hard and costly to obtain. It is common in practice to introduce the transmissivity which is the product of the hydraulic conductivity and the thickness of the water-saturated zone in the soil layer in which the flow takes place hence bypassing the difficulty of determining the thickness of the water-bearing zone. The water flux is then defined as the amount that passes through a vertical cross-section of unit width and height equal to the thickness of the water-saturated zone. The transmissivity is usually determined from a pumping test (Freeze and Cherry, 1979).

For a description of the groundwater reserve in an unconfined aquifer it is necessary to figure out the distributions of the water table height and the transmissivity in the horizontal plane. In this study, a local area in the northern part of Pohang, Kyungbuk, is chosen and the distributions of the head and the log-transmissivity are constructed by a geostatistical method. The results are displayed on a digital map of the area. The Rural Development Corporation, Ministry of Agriculture, has carried out a field study in the region and measured the water table depths in natural condition and the transmissivity at several wells from pumping test (RDC, 1997).

In the subsurface exploration, statistical methods are frequently adopted for the purpose of interpolating limited data to construct the distributions in space. Kriging is a popular method and has been applied in the mining industry for ore deposits and others (Gelhar, 1993). Its acronym is BLUE (Best Linear

Unbiased Estimator) since it preserves the measured data precisely in the process of interpolation unlike in other regression methods (Isaaks and Srivastava, 1989). In this study, kriging is applied to the finite set of data for the water table height and the log-transmissivity (rather than the transmissivity itself) to construct their spatial distributions in the horizontal plane. In kriging, the parameters of interest are defined as random variables and their characteristics in terms of variation in space with separation distance from a selected reference point are described by variogram. The experimental variogram is calculated from the available data and is approximated by a model which is then used for the interpolation. It is assumed in this study that the variograms are stationay and statistically homogeneous so that the variogram depends only on the separation distance and not the direction of the distance.

The results of kriging analysis of the water table height and the transimissivity are displayed on a digital map of the site, for a clear and convenient presentation in connection with such geographic information as the ground surface elevation, and the roads and streams. The map used here has been produced as a result of the National Geographic Information System (NGIS) project conducted by National Geographic Institute, Ministry of Construction and Transportation (NGI, 1996).

STUDY SITE

The wells at which the water level in natural condition was measured are distributed over a wide area that includes Heunghae-eub, Shinkwang-myun, Songrah-myun and Cheongha-myun in the northern part of Pohang. Their locations range approximately from 129°14′0″E to 129°23′0″E and from 36°5′0″N to 36°15′0″N. Contours for the ground elevation measured from the sea level are shown in Figure 1. Also shown are the major roads in double lines and streams. The wells are marked by solid circles. For a bird's eye view of the area, a three-dimensional plot of the ground surface is produced in Figure 2 in which the distances measured from the origin (129°14′0″E and 36°5′0″N) have been converted to km by using the fact that the interval of 1°corresponds to the horizontal distance of 90.166km in the south-north direction and 110.96km in the east-west direction respectively (Han, 1996). The northwest part has the highest elevations over 200m and there is an array of peaks in the south-north direction in the middle. In the eastern seaward part, the ground elevation is a few tens of meters except a few peaks of intermediate elevation.

As shown in Figure 1, the wells in the southwest part are located in a region where the variation of ground elevation is relatively high. In this study, the eastern part (6-13km in the east and 3-21km in the north as measured from the origin and is shown as a box in Figure 1) is chosen for a statistical analysis of the water table height, log-transmissivity and the flow field because the wells are more evenly distributed and the variation of the surface elevation is relatively mild. The wells used in the analysis are listed in Table 1 with the water table height and the log-transmissivity.

Pumping tests have been carried out in all of these wells with well depth ranging from 100m to 200m except a few for which the depth

exceeds 200m. No explosive out flushing after boring has been reported and the water level in the wells went down rapidly as soon as pumping started which is typical with pumping test in unconfined aquifers. An aquifer is a soil layer that bears groundwater with variable saturation. Hence the aquifers in the region are treated as phreatic (unconfined) ones and the water table height is a direct measure of the hydraulic head in the region

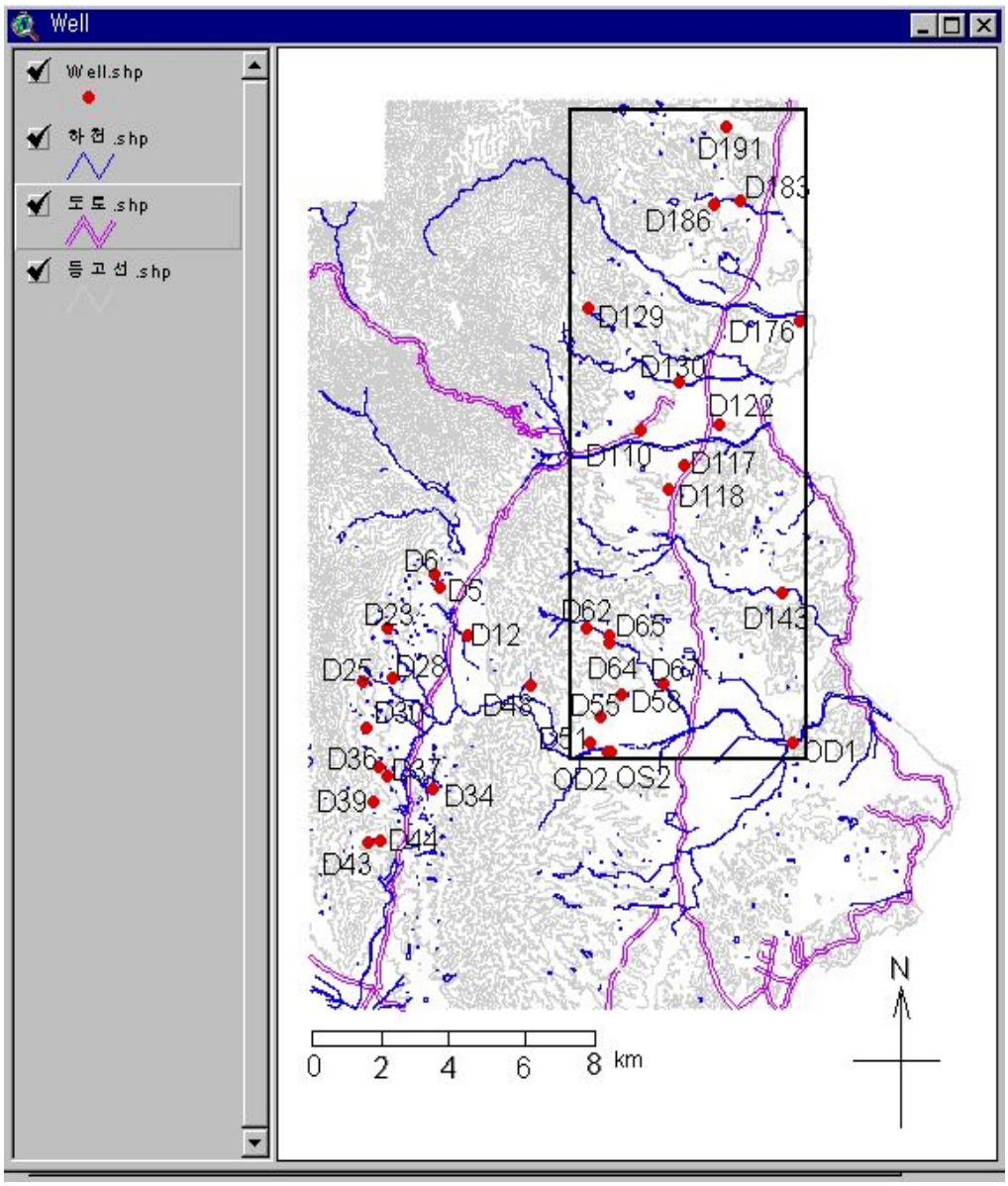

FIGURE 1. Area map with the observation wells marked by solid circles. Major roads are shown in double lines. Streams are also shown.

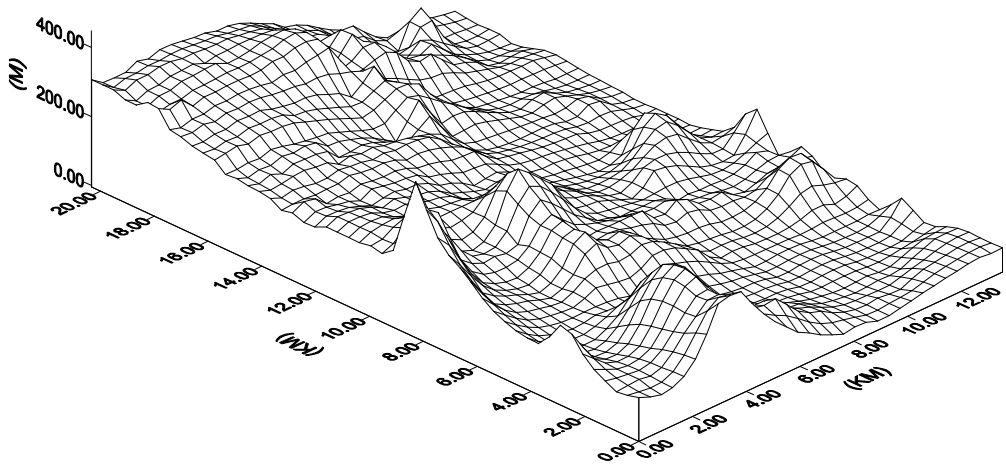

FIGURE 2. A three-dimensional plot of the ground surface for the area.

TABLE 1. The water table height and log-transmissivity values measured at the wells and the times of measurement.

Symbol	Water table height(m)	Log-transmissivity	Date 1996	Symbol	Water table height(m)	Log-transmissivity	Date 1996
D51	25.0	1.98	10/5	D122	21.7	1.44	10/19
D55	37.0	1.30	10/7	D129	103.1	1.68	10/19
D58	26.0	1.44	10/6	D130	29.8	1.31	10/20
D62	52.0	1.41	10/7	D143	6.0	0.66	10/20
D64	42.2	1.25	10/8	D176	3.4	-0.11	10/22
D65	42.0	1.46	10/10	D183	14.0	1.25	10/22
D67	30.8	1.34	10/10	D186	23.5	1.22	10/23
D110	48.5	1.19	10/17	D191	22.5	1.11	10/23
D117	23.0	1.06	10/17	OD1	40.7	0.64	11/6-10
D118	33.0	2.19	10/18	OS2	23.0	1.16	11/18-23
				OD2	24.6	0.92	11/11-17

METHODS OF ANALYSIS

The distributions of water table height and log-transmissivity in the study area are constructed as follows:

1. Collect the values of the water table depth from the ground surface and the transmissivity measured from the wells.

2. Obtain the water table height by subtracting the water table depth from the ground elevation, and the log-transmissivity by taking the natural logarithm of the transmissivity.
3. Use the geostatistical analysis package Geo-EAS (Englund and Sparks, 1991) to carry out kriging analysis of the variables at the nodes of square grid system with spacing 0.5km.
4. Import the results into ArcView and convert the horizontal coordinates x and y given in deg./min./sec. to the Transverse Mercator (TM) coordinates.
5. Use the contour option for the water table height and log-transmissivity data and display them over the digital map.

The flow field is determined by using depth-integrated Darcy's law and finite differences with the water table height and transmissivity obtained in Step 3 above with second-order accuracy.

DISTRIBUTION OF WATER TABLE HEIGHT

Using the data in Table 1, the distribution of water table height from the mean sea level is constructed over the region by kriging. Variogram plays the central role in interpolations with kriging, and shows the varying trend of the variable, which is assumed to be random, with distance vector $\boldsymbol{h}$ between two separate points.

A brief description of variogram is given here. The variogram, in principle, depends on the location $\boldsymbol{x}$ at which the current origin of reference is placed and the distance vector $\boldsymbol{h}$ and the variogram $\gamma_{yy}(\boldsymbol{x}, \boldsymbol{h})$ for a random variable $Y(\boldsymbol{x})$ is defined as

$$\gamma_{yy}(\boldsymbol{x}, \boldsymbol{h}) = \frac{1}{2} E\{[Y(\boldsymbol{x}+\boldsymbol{h}) - Y(\boldsymbol{x})]^2\} \quad (1)$$

where $E[\cdot]$ is the expectation. However in many practical situations, the variogram appears to be nearly independent of $\boldsymbol{x}$ (stationary) and also independent of the direction of the vector $\boldsymbol{h}$ (statistically isotropic). It is assumed here that the data set investigated satisfies these conditions. The variogram then becomes

$$\gamma_{yy}(h) = R_{yy}(0) - R_{yy}(h) \quad (2)$$

in which the distance is characterized by its magnitude only and is denoted by a scalar quantity h. The symbol $R_{yy}(h)$ denotes the covariance function.

Theoretically $\gamma_{yy}(h \to 0) = 0$ but, due to the lack of data for sufficiently small h and possibly some measurement error, $\gamma_{yy}(h)$ sometimes does not go to zero as h goes to zero and this non-zero limit is known as nugget. When $\gamma_{yy}(h)$ approaches a constant value as h goes to infinity, the limit value subtracted by the nugget is called the sill and the value of h when this limit value is reached with increasing h is called the range.

The experimental variogram for the watertable height has been calculated from the data in Table 1 by Lee and Moon (1999) and is reproduced in Figure 3. The values are shown by the asterisks (*). Although the trend of the variogram for the values of h greater than 6 is not very clearly exhibited, the variogram is modeled as a spherical variogram with nugget zero and is written as

$$\gamma(h) = \omega\left[\frac{3}{2}\left(\frac{h}{a}\right) - \frac{1}{2}\left(\frac{h}{a}\right)^3\right] \quad (h < a) \quad (3\text{-}1)$$

$$\gamma(h) = \omega \quad (h > a) \quad (3\text{-}2)$$

where ω and a are the sill and range

respectively. The range has been chosen as 6 and the sill has been determined upon minimizing the error of approximating the discrete variogram data by (3-1) and (3-2) by regression and turned out to be 596. The model variogram is plotted as the curve in Figure 3. By using this variogram model, block kriging has been carried out over the region to find the interpolated estimate of the water table height at two-dimensional array of small blocks in the horizontal plane.

The results of kriging of the water table height are shown as contours in Figure 4. The levels are separated by 5m. It is cearly shown that the water table height decreases primarily toward the east from the large peak located in the northwest region and also from an intermediate peak in the southwest region. It also shows gradual decrease in the southward direction from the peaks.

DISTRIBUTION OF LOG-TRANSMISSIVITY

In most aquifers, the stratigraphy of the region of interest is not well known and it is hard to obtain the spatial distribution of the aquifer thickness at a reliable level. Seismological survey of the region is sometimes employed. On the other hand, aquifers, although their thickness varies in space sometimes quite substantially, it is common practice to determine the transmissivity which is the product of the hydraulic conductivity and the aquifer thickness from pumping test. Under the assumption (Dupuit assumption) that the water table and the bottom boundary of the aquifer change slowly in the horizontal plane, the groundwater flow is often described by the two-dimensional depth-averaged flow equation. Hence the transmissivity is the most important parameter that reflects the hydrogeological

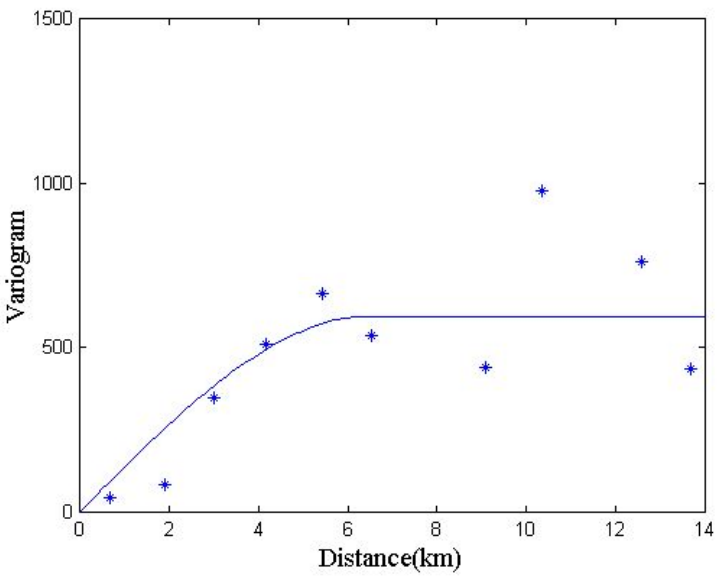

FIGURE 3. Variogram for water table height and a spherical model with nugget=0, sill=596, and range=6.

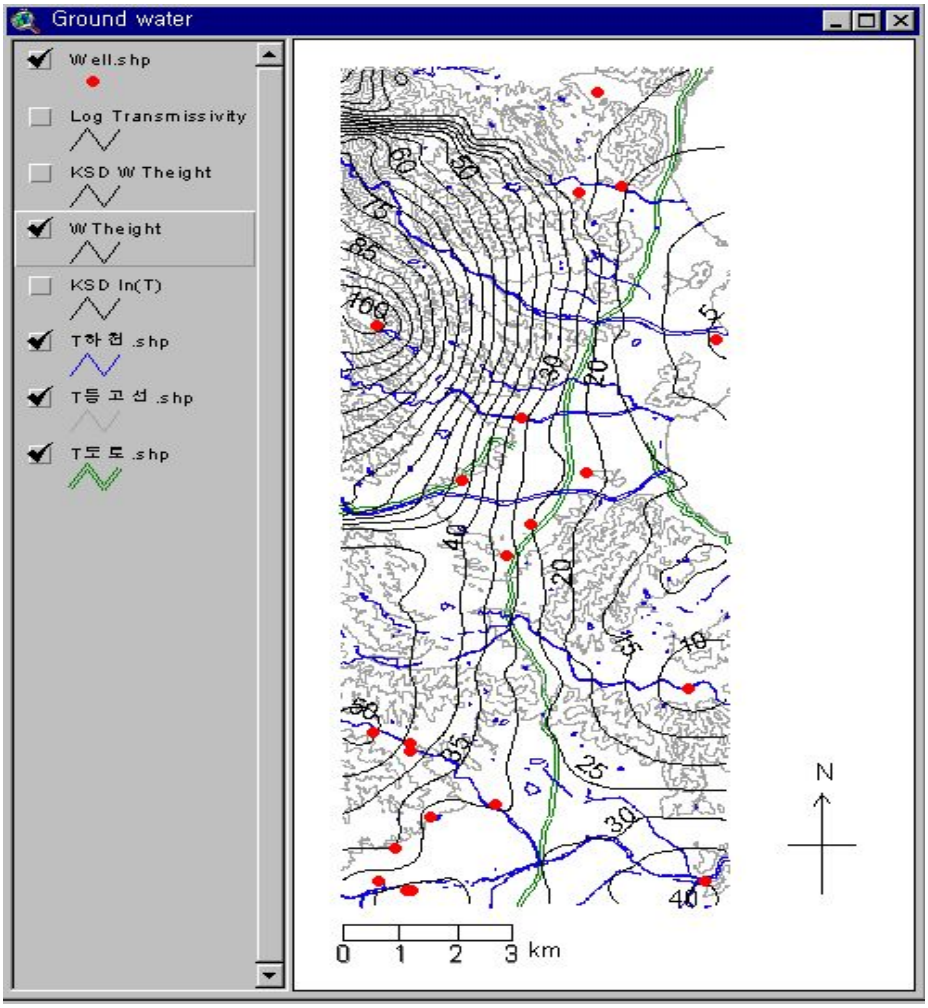

FIGURE 4. Distribution of the kriged water table height measured from the sea level in meters.

characteristics of an aquifer system. The flow equation is then written as

$$\nabla \cdot (T\nabla\phi) = \frac{\partial}{\partial x}\left(T\frac{\partial\phi}{\partial x}\right) + \frac{\partial}{\partial y}\left(T\frac{\partial\phi}{\partial y}\right) = 0 \quad (4)$$

where ∇ is the two-dimensional gradient operator in the horizontal xy-plane and ϕ and T are the hydrauluic head and the transmissivity respectively. Equation (4) may be written

$$\nabla^2\phi + \frac{\nabla T}{T}\cdot\nabla\phi = \nabla^2\phi + \nabla(\ln T)\cdot\nabla\phi$$
$$= \left(\frac{\partial^2\phi}{\partial x^2} + \frac{\partial^2\phi}{\partial y^2}\right) + \left[\frac{\partial(\ln T)}{\partial x}\frac{\partial\phi}{\partial x} + \frac{\partial(\ln T)}{\partial y}\frac{\partial\phi}{\partial y}\right] = 0 \quad (5)$$

which suggests that the logarithm of the transmissivity ($\ln T$) be treated as a random variable independent of the hydraulic head ϕ. It has been frequently demonstrated that the distribution of log-transmissivity exhibits the

normal distribution rather closely than the transmissivity itself does (Gelhar, 1993).

Transmissivity values have been determined at the wells listed in Table 1 from pumping test. It is valid under the assumptions mentioned earlier for treating the groundwater flow effectively in two-dimensional manner. They are shown in the third columns of the left and right parts in Table 1 as log-transmissivity. In stochastic approaches in the underground environment, due to uncertainties and limitations of available data, the transmissivity (or the hydraulic conductivity and the aquifer thickness) is taken as another random variable independent of the hydraulic head. We have chosen the log-transmissivity as the variable of interest and carried out kriging analysis of it.

The calculated variogram for the log-transmissivity is shown in Figure 5 by * symbol. Although scattering of the experimental variogram beyond the distance of 6km is somewhat large, a spherical variogram is chosen with a nugget of zero, a sill of 0.287, and a range of 6 to represent the experimental one. The model is shown as a curve in the same figure. Again the fitting has been made by a regression method that minimizes the error, which is the sum of the square of the differences between the model and the calculated ones.

Kriging of the log-transmissivity is conducted at a spatial interval of 0.5km in both the eastern and northern directions so that there are 15 nodes along the east and 37 nodes along the north. The results of kriged log-transmissivity are shown as contour lines in Figure 6. It reaches the maximum of about 2 in the central part of the region and decreases gradually toward the boundary.

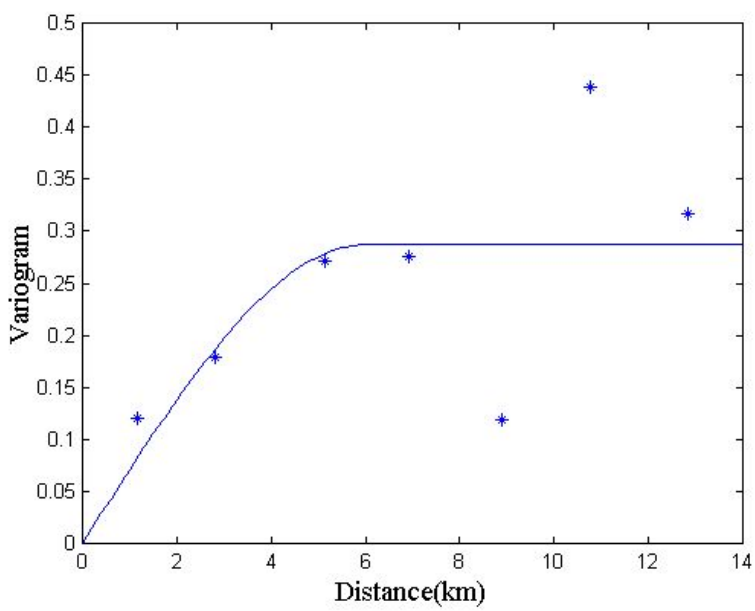

FIGURE 5. Variogram for the log-transmissivity data and a spherical model with nugget=0, sill=0.287 and range=6.

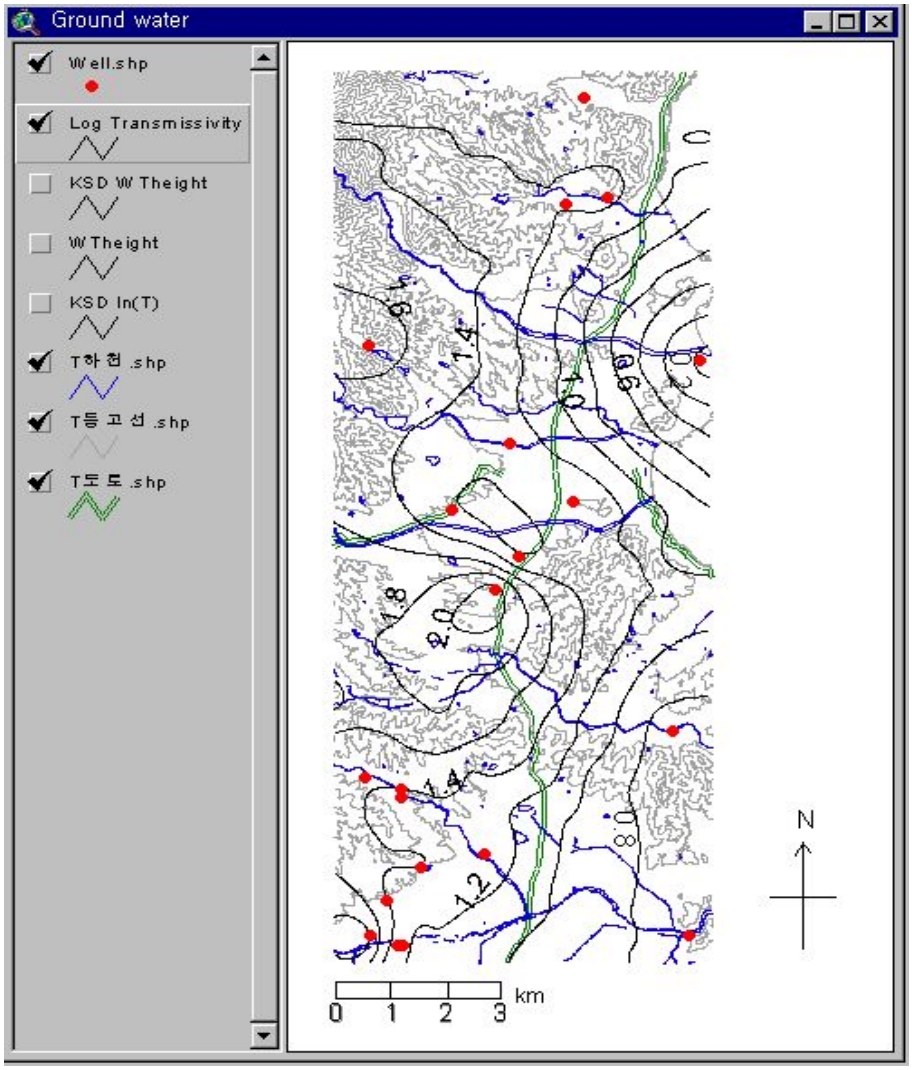

FIGURE 6. Distribution of kriged log-transmissivity

DEPTH-INTEGRATED FLOW FIELD

The distributions of the hydraulic head (or the water table height in an unconfined aquifer) and the log-transmissivity have been constructed by kriging in the previous sections together with kriging standard deviation (not shown in this article). Although there exists certain level of uncertainties in the kriged values of the head and transmissivity, it is yet useful to use the interpolated distributions to calculate the water flux across a vertical soil cross-section. Integrating Darcy's law over the cross-section, the flow rate across a vertical cross-section which has unit horizontal width and the height equivalent to the local thickness of the saturated zone in an unconfined aquifer is given by the product of the transmissivity T and

the hydraulic gradient $\nabla\Phi$.

Finite differences with $O(\Delta^2)$ consistency, where Δ is the typical spacing between nodes, are employed to calculate the flow field due to the anomalies of hydraulic head and transmissivity. The node spacing has been chosen as 0.5km identically in both the east-west and the south-north directions. Hence the region is discretized by square grids with 14 intervals in x and 36 intervals in y. The following has been used to calculate the x (west-east)- and y (south-north)-direction flow rates.

$$q_x = -T\frac{\partial\Phi}{\partial x};$$
$$(q_x)_{i,j} = -T_{i,j}\frac{\Phi_{i+1,j}-\Phi_{i-1,j}}{2\Delta} + O(\Delta^2) \qquad (6.1)$$

$$q_y = -T\frac{\partial\Phi}{\partial y};$$
$$(q_x)_{i,j} = -T_{i,j}\frac{\Phi_{i,j+1}-\Phi_{i,j-1}}{2\Delta} + O(\Delta^2) \qquad (6.2)$$

where the set of subscripts $(\cdot)_{i,j}$ implies that the quantity is defined at the node x_i and y_j. The truncation error associated with the central difference in (6.1) and (6.2) is estimated to be of 0.5% or less of the overall variation rate. For example, a variation of $O(1)$ is over the distance 7km in x-direction and the error due to discretization over a node spacing of 0.5km is approximately $(0.5/7)^2 = 0.005 = 0.5\%$. If the point is located on the boundary, either the forward or backward difference is used, i.e. $(\partial\Phi/\partial x)_{i,j} = (-3\Phi_{i,j}+4\Phi_{i+1,j}-\Phi_{i+2,j})/(2\Delta) = (3\Phi_{i,j}-4\Phi_{i-1,j}+\Phi_{i-2,j})/(2\Delta)$, both of which are $O(\Delta^2)$ accurate. Similar expressions for $(\partial\Phi/\partial y)_{i,j}$ are used. The algebra is straightforward.

The calculated flow field is shown in Figure 7 with arrows. To avoid unnecessary confusion with the background information, it is shown separately. The reference arrow is also shown for the magnitude of 0.1 $m^2/\sec$. in the lower part. As implied in the distribution of the hydraulic head in Figure 4, the flow is dominantly in the east which is roughly the same direction as the overall decrease of the ground surface elevation in the region (see Figure 2). Obviously the maximum flow rate occurs where the product of the transmissivity and the hydraulic gradient $\nabla\Phi$ becomes maximum. The maximum flow rate appears on the eastern hillside of the water table peak. It should be noted however that the local variations of the hydraulic head and the transmissivity are hardly correlated to the ground surface variation although the overall variation of the head over the regional scale is roughly the same as that of the ground surface. Accordingly the change of the ground elevation should not be used to provide a clue to finding the flow pattern.

DISCUSSION

The water table height (Figure 4) shows steady decrease in the western part toward the east and south due to a large peak with the elevation from sea level of 100m in the northwesttern part. In the eastern part of the region, the same trend continues toward the sea at a moderate rate except the southeastern corner where a mild water table peak (40m high from the sea level) exists. As a result the flow direction in that corner appears to be in the north and west respectively on the northern and western sides of the mild peak although the magnitude is very small (Figure 7).

Two factors most directly influence the flow field: the hydraulic gradient and the transmissivity. The hydraulic gradient $\boldsymbol{J} = \nabla\Phi$ has the components $J_x = \partial\Phi/\partial x$ and $J_y = \partial\Phi/\partial y$ in

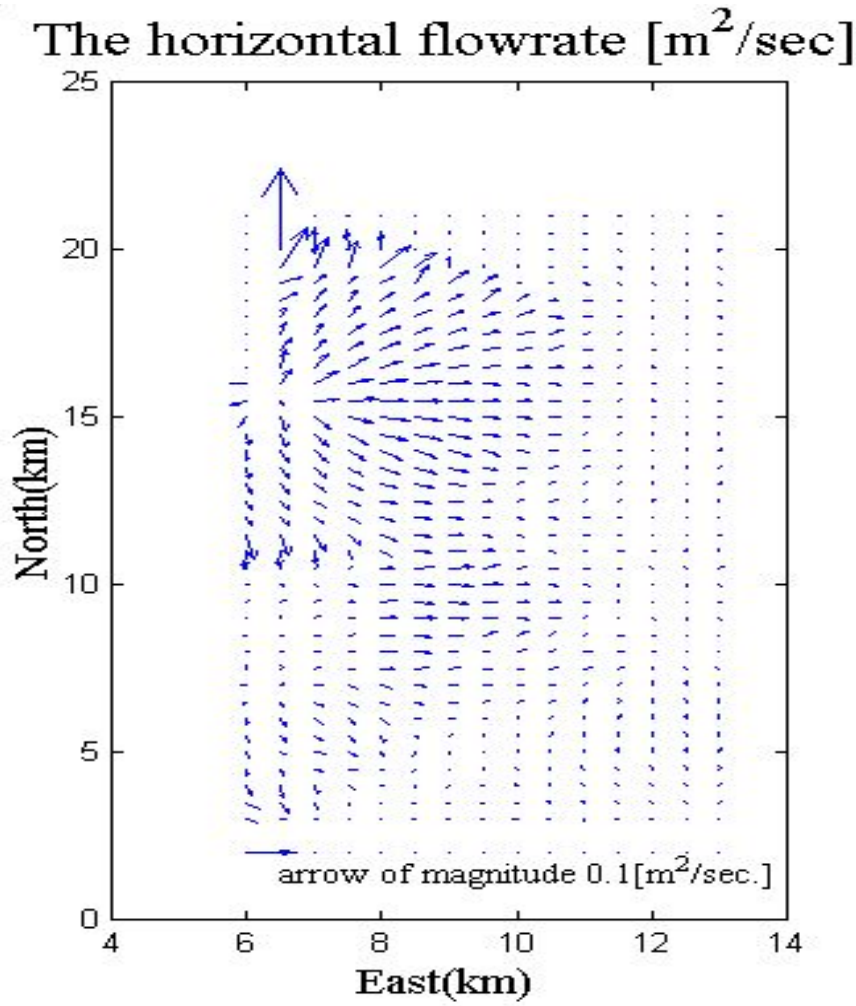

FIGURE 7. Flow field calculated from the hydraulic head and the transmissivity.

the unconfined aquifer investigated here. The x-direction component J_x becomes maximum at about 0.013 on the eastern hillside of the major peak in the northwest. It is usually in the range of 0.0001 to 0.001 in the rest part of the region. This implies that the maximum downsloping is at most 1% or so and is otherwise nearly flat meaning highly stable in general. The y-direction component J_y is about 0.03 on the north side and 0.01 on the south side of the major peak, but the value on the north side close to the upper boundary is not very reliable because the kriging has been omitted around the boundary north to the peak. In the rest of the region, similar to J_x, the magnitude of J_y stays in the range of 0.0001 to 0.001.

The log-transmissivity also shows nearly

monotonic decrease from around 2.0 in the central part of the region roughly radially becoming 1 or less near the boundary. Note that the log-transmissivity shows a mild slope in the northern half toward the east where the highest water table height has been identified in the west. This implies that the relatively large $\ln(T)$ at the location is most probably due to, recalling that the transmissivity is the product of the hydraulic conductivity and the thickness of the water-bearing zone, large thickness of the saturated zone in the aquifer. Note also that the $\ln(T)$ is becoming nearly zero (transmissivity becoming very large negative number) on the right boundary at about two-thirds north. In fact, that little spot is off the beach and belongs to the East Sea and hence trnasmissivity is not defined.

The flow rate magnitude is mostly less than $0.5\ m^2/\sec$ except around the water table peak where it becomes $0.7\ m^2/\sec$ or larger. The big arrows in the far northwestern corner are not to be taken seriously because the kriging has been omitted at the boundary. Note that the arrows show a diverging trend on the east hillside of the peak whereas they show turning trend otherwise, i.e. the flow direction rotates to the right in the northeastern part of the peak and to the left in the southeastern part of the peak respectively as it advances. This implies that a groundwater contamination, usually in the form of cloud in the aquifer is to spread wide laterally in the eastern hillside while it is being tranported by the groundwater flow. Of course there will be longitudinal spreading due to dispersion. It is also shown that there exists converging regions at (9km E, 9km N) and (7km E, 4km N) where it is anticipated that the transport pattern there is not going to induce significant spreading laterally.

The regional averages of J_x and J_y have been calculated by taking the arithmetic mean of the values at the nodes. The average values are -1.6×10^{-6} and -1.7×10^{-7} for J_x and J_y respectively. On the other hand, the regional mean hydraulic gradient is shown to be oriented -174 degrees counterclockwise from the east confirming that the dominanat direction is in the east.

CONCLUSIONS

The digital map with the major roads and streams from the NGIS project has been used as the background information to present the results of delineating the ground water table height, the log-transmissivity, and the flow field caused by the hydraulic head anomaly. A few conclusions are drawn from the present study and analysis:

1. The digital map serves as a convenient tool for displaying the results of investigation in that the primary geographic features such as ground elevation, roads, and streams are shown together.
2. The water table height variation is primarily a decreasing pattern from the west to the east roughly in the same trend as that of the overall ground surface elevation.
3. The log-transmissivity shows the maximum level in the central part of the region and a decreasing pattern outwardly.
4. The flow field shows outward diverging trend from the peak of the water table height in the northwest and is dominantly in the direction from the west to the east.

CONCLUDING REMARKS

It is important, in the ground water resource management, to construct the distribution of the hydraulic head and transmissivity in a reliable manner. Of more importance and interest is to construct such distributions that are clearly depicted in geographic space so that the selection of future ground water development for agricultural and/or industrial purposes and the identifications of severe depletion of or contamination of ground water can be promptly and efficiently made. Digital maps provide valuable background information for planning any such projects.

ACKNOWLEDGMENT

The present study has been supported by the Korea Research Foundation under the contract to the Geographic Information System (GIS) Institute at Handong University for 'A Study of Groundwater Management System by Utilizing GIS and Groundwater Modeling' in the year of 1999. The financial support is gratefully acknowledged. The author would like to express thanks to Mr. T. W. Ahn in the School of Construction, and Urban Environmental Engineering, Handong University for preparing Figures 1, 4, and 6.

REFERENCES

Bear, J. 1972. Dynamics of Fluids in Porous Media. Dover Pub., Inc., 764pp.

Englund, E. and A. Sparks. 1991. GEO-EAS 1.2.1. Geostatistical Environmental Assessment Software. Environmental Monitoring Systems Laboratory, Las Vegas, NV, USA.

Freeze, R.A. and J.A. Cherry. 1979. Groundwater. Prentice-Hall. 604pp.

Gelhar, L.W. 1993. Stochastic subsurface hydrology. Prentice-Hall. 390pp.

Han, G.H. 1996. Principles of cartography (in Korean). Mineumsa. 387pp.

Isa만, E.H. and R.M. Srivastava. 1989. Applied geostatistics. Oxford Univeristy Press. 561pp.

Lee, C.K. and C.Y. Moon. 1999. Estimation of ground water table using well data and GIS digital map (in Korean). submitted.

National Geographic Institute (NGI). 1996. 1:5,000 digital map of the city of Pohang.

Rural Development Corporation (RDC). 1997. Areal distribution of groundwater in Yeongchung area. Rep., RDC, Ministry of Agriculture (in Korean).